Computational Study on the Effect of the Pulse Length on Laser Ablation Processes

"Stefan Tatra *, Rodrigo Gómez Vázquez, Andreas Otto"

"Vienna University of Technology, Institute for Production Engeneering and Laser Technology, Getreidemarkt 9 1060 Wien, Austria"

Abstract

Laser assisted ablation technology is widely used for micro-fabrication of metal and semiconductor components in the electronic industry. The outcome of those processes strongly depends on several variables such as the used material and different laser parameters. For a better understanding of these processes a study on the effect of the pulse length based on multi-physical simulations was performed. The use of a complex model which extends original CFD-capabilities of OpenFOAM simulation software with multiple physics allows us to obtain detailed description of the phenomena taking place during the process. Special attention is paid to transient process characteristics including melt ejections and metal vapor dynamics as well as ablation depth and their dependency on the pulse length scales applied. The limitation of the model, especially at ultra short pulses, is analyzed and possible improvements are discussed. Apart from the computational investigation comparison of simulated results against available experimental data is finally provided.

Keywords: multi-physical simulations; laser ablation; volume of fluid;

1. Introduction

Numerical simulation is an important tool both for industrial and in scientific research. Simulations do not only allow a view inside the work piece, but they also help to get a better understanding of the experimental

---

* Corresponding author. Tel.: +43-1-58801-311627; fax: 43-1-58801-9-311611.
E-mail address: stefan.tatra@tuwien.ac.at.

processes, due to the possibility to examine the influence of single process parameters on the whole process, and can therefore be used for the planning of steps in a production line or even the whole production chain.

Even though there already were investigations and comparisons of laser ablation with different pulse lengths before [Leitz et. al., 2011, Shaheen et. al., 2013], these experiments' parameters differed in more than just the pulse length. Therefore in our simulations the laser ablation of iron with three different pulse lengths and otherwise equal parameters was compared.

1.1. Simulation Model

The simulations were performed with a solver based on OpenFOAM, a C++ based numerical simulation toolbox. The solver considers beam-matter interaction as well as phase changing and fluid dynamics. It's based on the finite volume method and uses the volume of fluid method approach [Hirt and Nichols, 1981]. Apart from fluid dynamics, propagation of the laser beam, absorption respectively multiple reflections of the laser beam and thermo dynamical effects such as heat transfer and phase changes which are described in [Otto et. al., 2012], this model also incorporates plasma development and the respective absorption of the laser beam.

For the simulation of plasma shielding a method first published by [Mahrle and Beyer, 2006] and later on also used in [Dasgupta et. al., 2007] has been integrated into the model. The electron density is calculated by

$$n_e = \frac{\chi p}{kT},$$

(1)

where n_e is the electron density, χ is the ionization grade, p is the pressure and k is the Boltzmann constant. The ionization grade is calculated with the Eggert-Saha equation

$$\frac{\chi^2}{1-\chi} = \left(\frac{2\pi m_e}{h^2}\right)^{\frac{3}{2}} \frac{(kT)^{\frac{5}{2}}}{p} \exp\left(-\frac{E_i}{kT}\right).$$

(2)

Hereby m_e is the electron mass h is the Planck constant and E_i is the ionization energy. This equation only takes into account the first ionization, thus surely underestimates the amount of free electrons within the plasma plume and thus absorption due to inverse Bremsstrahlung.

The plasma absorption coefficient α [Hughes, 1975; Paulini and Simon, 1993] is calculated by

$$\alpha = \frac{n_e^2 e^6}{6\sqrt{3}\mu\varepsilon_0^3 c\hbar\omega^3 m_e^2}\left[1-\exp\left(\frac{-\hbar\omega}{kT}\right)\right]\left(\frac{m_e}{2\pi kT}\right)^{\frac{1}{2}}\overline{g},$$

(3)

where e is the electron charge, μ is the real part of the plasma refractive index ε_0 is the permittivity of vacuum, c is the speed of light, $\hbar$ is the reduced Planck constant, ω is the laser frequency and $\overline{g}$ is the average Gaunt factor, which is set to one due to reasons of simplicity. The resulting plasma absorption coefficient is used in our beam propagation and ray tracing module that has already been explained in [Otto et

al., 2012]. This model is quite similar to the one that has been proposed by [Ki et. al., 2002; Cho and Na, 2006].

As we have to deal with extreme temporal and spatial temperature gradients, we divide the energy equation into two parts. First we calculate the convective heat transport by means of solving equation 4

$$\frac{\partial \rho H}{\partial t} + \nabla \cdot \left(\rho \vec{u} H\right) = Q. \tag{4}$$

From the resulting enthalpy H we calculate the latent heats for fusion and evaporation L and derive the temperature T using equation 5

$$c_p \times \left(T - T_0\right) = H - L. \tag{5}$$

Finally we solve the conductive part of heat transport equation 6

$$\rho c_p \frac{\partial T}{\partial t} = \nabla\left(\lambda \nabla T\right), \tag{6}$$

and correct the energy distribution with respect to heat conduction. In equations 4 to 6 H is the specific enthalpy, t is the time, ρ is the density, u is the velocity, Q is the absorbed energy, L is the latent heat and cp is the specific heat. Non linear heat conduction phenomena that are important at very short time scales (for ultra short laser pulses) are not yet implemented but will be dealt with in the next future.

Fluid mechanical effects are described by the Navier-Stokes equations. For this purpose we developed a new method to take into consideration compressibility that cannot be explained in detail at this point.

2. Simulation study

Simulations of laser ablation with three different pulse lengths, one in the range of nano-, one in the range of pico- and one in the range of femtoseconds, were performed. Iron was chosen as work piece material.

2.1. Parameters and initial conditions

The simulations were performed with three different pulse lengths. The remaining parameters were kept unmodified. In table 1 the chosen process parameters are shown. Both the local and temporal shape of the laser beam was considered Gaussian.

Table 1: Process parameters

Parameter	Symbol	Value
Laser wavelength	λ	532nm
Focus radius	r	20μm
Pulse frequency	f	120kHz
Pulse length	τ	60ns, 10ps, 170fs
Pulse energy	E	280μJ

2.2. Simulation results

Figure 1 shows the ablation result after 25 pulses for nano- , pico- and femtosecond ablation with the parameters given in table 1. The colors indicate the amount of liquid at the end of the pulse. For nanosecond pulses we get a closed liquid film on the surface of the ablation crater that is driven outwards by means of the recoil pressure of the evaporating material. Due to surface tension the liquid mass flow is decelerated at the top of the crater and forms a quite significant burr. Both for pico- and femtosecond pulses the amount of liquid is much less. The ablation process is mainly driven by the direct evaporation of the material though still molten material and also the development of droplets and burr can be observed.
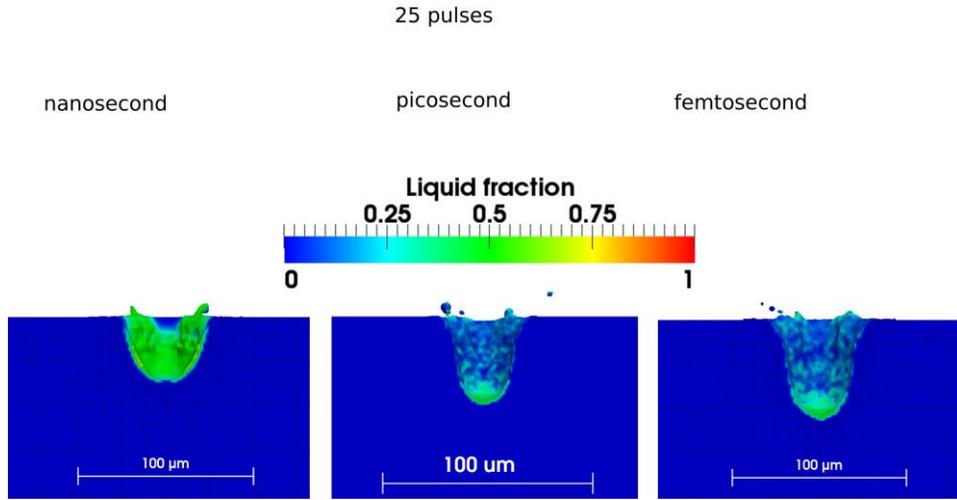

Fig. 1. Comparison of the simulation results for the three different pulse lengths after 25 pulses. From left to right: femto-, pico- and nanosecond pulses.

Despite of the similarities in the processes it can be noticed that the ablation depth and also the amount of ablated material after 25 pulses is slightly smaller for nanosecond pulses (see table 2). Obviously the ablation efficiency calculated with the model is nearly the same for pico- and femtosecond pulses, while significantly reduced for nanosecond pulses. This effect can be easily explained as the influence of plasma shielding can be neglected for the very short pulses and plays a significant role for the longer nanosecond pulses.

Table 2: Quantitative results of the simulation for different pulse lengths

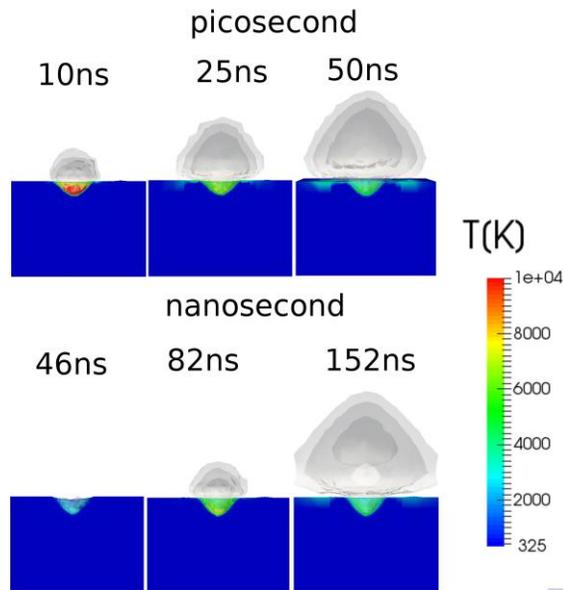| Pulse length	Number of pulses	Ablation depth[μm]	Ablated mass[ng]
60ns	25	37.5	277
10ps	25	53	394
170fs	25	53	376

Fig. 2. On top: picosecond pulses 10, 25 and 50ns after pulse begin. On bottom: nanosecond pulses 46, 82 and 152ns after pulse begin. The contours above the surface represent the metal vapor respectively plasma with from inside to outside 20000, 10000 and 5000K.

In figure 2 the evolution of the metal vapor is shown. It is evident, that in case of the shorter pulses vaporization doesn't start during the pulse but a few nanoseconds afterwards, although the irradiated spot is already heated above the boiling temperature of iron. Compared with that in the case of nanosecond pulses, vaporization starts during the pulse, thus also plasma heating and shielding begins. From the simulation results it can be estimated that roughly 30% of the laser power is absorbed within the developing plasma plume for nanosecond pulses. However, in absolute time, vaporization starts faster with picosecond pulses. While 46ns after pulse begin vaporization with nanosecond pulses has just started and we see only the contours for 5000 and 10000K in figure 2, with picosecond pulses the contour of 20000K is already quite pronounced at 10ns after pulse begin.
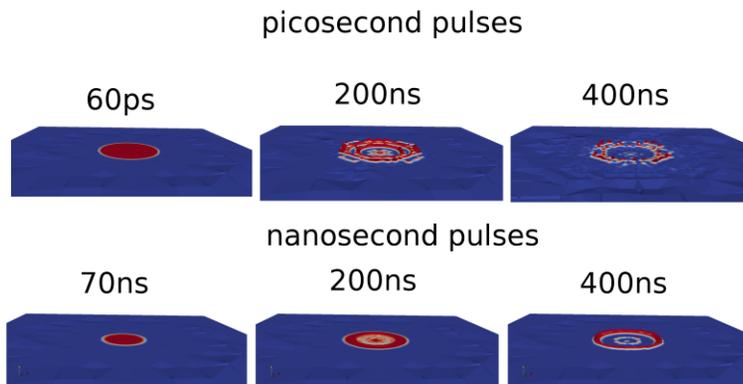

Fig.4. Spreading of molten material after the begin of the first pulse

In Figure 4 the spreading of the molten material after the first pulse is shown. The picosecond pulses take about 60ps for the maximum of melting which is 6 times the pulse length. This can be explained with the fact, that the pulse time is shorter than the time needed for the heat conduction. After about 3ns vaporization starts and begins to press the molten metal from the center of the spot outwards. In case of nanosecond pulses a significant amount of the melting takes place during the pulse. The displacement of the molten phase due to the recoil pressure starts at about 90 ns after pulse begin, even though it takes only about half this time until the start of vaporization.

The results presented in this section obviously don't match with the common theory and experimental results that a shorter pulse length causes less ablation, e.g. [Leitz, 2012]. Thus we compared the simulation results with experiments.

2.3. Model validation

Simulations were made with the same parameters as in the nanosecond experiments of [Leitz, 2011], which are 60ns pulse length, 280μJ pulse energy and a pulse repetition rate of 120 kHz. Figure 5 shows the simulation results after 50 pulses. The ablation depth of about 55 nm, as well as the diameter of the crater and the ejected mass fits well with the experimental results. Even the burr development can be seen in the simulation results.
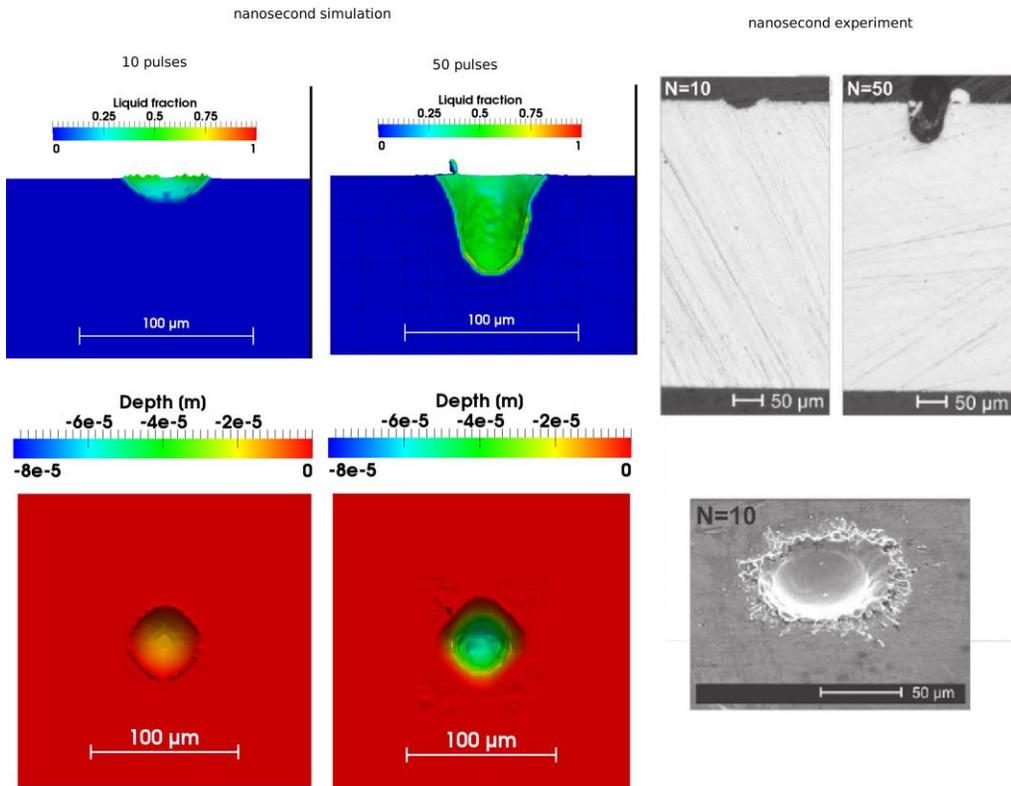

Fig.5. Nanosecond laser ablation: Comparison between simulation and experiment. The pictures of the experiment are from [Leitz, 2011]

Obviously there is an excellent agreement between simulation and experiment in the case of nanosecond pulses both qualitatively and quantitatively. However, when we compare the simulation results for femtosecond pulses with experiments we get strong deviations. Simulations were again made with the same parameters as in the femtosecond experiments of [Leitz, 2011], which are 170fs pulse length, 300µJ pulse energy and a pulse repetition rate of 1kHz.

The ablation depth in the simulation is strongly overestimated by a factor of about 4. This is due to the neglecting of the effects that take place at very short time scales, namely the electron-electron and electron-phonon interaction, which can be described by a two temperature model, and multi-photon absorption.
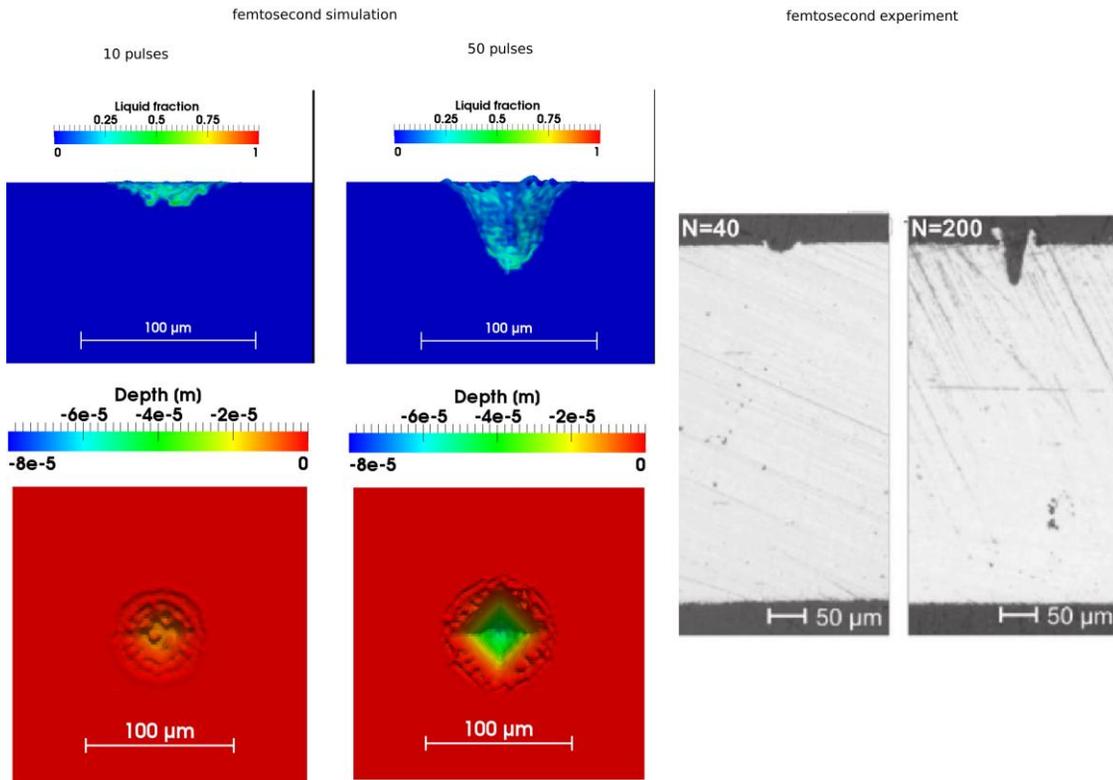

Fig.5. Femtosecond laser ablation: Comparison between simulation and experiment. The pictures of the experiment are from [Leitz, 2011]

3. Summary and Outlook

Our simulation model is capable to simulate laser material processing. Additional to the effects, already described by our previous models, which are absorption and reflection of the laser beam, heat transfer, phase changes and fluid dynamic effects, it takes into account plasma building, and shielding of the laser beam because of beam-plasma interaction.

In this paper a comparison between ablation with nano-, pico- and femtosecond pulses with the same pulse energy was shown. With nanosecond pulses there was less ablated mass than with pico- and femtosecond pulses, which both show nearly the same ablation rate. This effect can be explained by plasma shielding

effects that are important for longer pulses but can be neglected for short pulses. A comparison of results of experiments with simulations in the nanosecond case shows excellent agreement.

However the results of the femtosecond case do not fit well with experimental results. It is shown that the developed model overestimates the ablation rate for femtosecond pulses by a factor of about 4 for the conditions chosen within the experiments.

To further improve the model it is thus planned to include a two-temperature model for describing the electron-phonon-interaction.

References

Leitz, K. H., Redlingshöfer, B. ;Reg, Y.; Otto, A.; Schmidt, M.; 2011:Metal Ablation with Short and Ultrashort Laser Pulses. Physics Procedia 12, pp.230-238.

Shaheen, M. E., Gagnon, J. E., Fryer, B. J. , 2013: Laser ablation of iron: A comparison between femtosecond and picosecond laser pulses. Journal of Applied Physics 114, 083110.

Hirt, C. W.; Nichols, B.D.; 1981: Volume of fluid (VOF) method for the dynamics of free boundaries, Journal of Computational Physics 39 (1); p. 201.

Otto, A.; Koch, H. , Vázquez, R.G., 2012: Multiphysical simulation of laser material processing, Physics Procedia 39, pp. 843-852.

Ki, H; Mohanty, P. S.; Mazumder, J.,2002: Multiple reflection and its influence on keyhole evolution. Journal of Laser Applications; Volume 14, Issue 1 pp. 39-45.

Cho, J.-H.; Na, S.-J.,2006: Implementation of real-time multiple reflection and Fresnel absorption of laser beam in keyhole. Journal of Phyics D: Applied Physics 39; p. 5372.

Mahrle, A., Beyer, 2006. Hybrid laser beam welding—Classification, characteristics and applications. Journal of Laser Applications 18, p. 169.

Dasgupta, A. K., Mazumder, J. Li, P., 2007. Physics of zinc vaporisation and plasma absorption during CO2 laser welding. Journal of Applied Physics 102, 053108.

Hughes, 1975. Plasma and laser light (Hilger, Bristol)

Paulini, J., Simon, G., 1993. Journal of Physics D 26, p. 1523.

Leitz,K.H., Koch, H., Otto, A., Schmidt, M.,2012. Numerical simulation of process dynamics during laser beam drilling with short pulses. Applied Physics A 106, pp. 885-891.